

Experimental Comparison of Performance Monitoring Using Neural Networks Trained with Parameters Derived from Delay-Tap Plots and Eye Diagrams

Xiaoxia Wu¹, Jeffrey A. Jargon², Chih-Ming Wang², Loukas Paraschis³, and Alan E. Willner¹

1. Dept. of Electrical Engineering - Systems, University of Southern California, Email: xiaoxia@usc.edu

2. National Institute of Standards and Technology, Boulder, CO 80305 USA

3. Optical Networking, Advanced Technology and Planning, Cisco Systems, Inc.

Abstract: We experimentally demonstrate the use of artificial neural networks trained with parameters derived from both delay-tap plots and eye diagrams for multi-impairment monitoring in a 40-Gbit/s non-return-to-zero on-off keying system.

©2010 Optical Society of America

OCIS codes: (060.2330) Fiber optics communications; (100.4996) Pattern recognition, neural networks.

1. Introduction

As data rates increase and network architectures become more complex, it becomes more difficult to predict and manage data impairments due to degradations that can change with time. In order to enable robust and cost-effective “self-managed” operations, optical networks will need to be able to agilely monitor their physical states and the quality of propagating data signals, automatically diagnose and repair problems, redirect traffic, and dynamically allocate resources. Thus, optical performance monitoring (OPM) and automatic system control are becoming increasingly important [1, 2]. Key features of optical performance monitors are simplicity in implementation and the ability to accommodate different modulation formats and impairments.

OPM can be performed by measuring changes to the data and determining “real-time” changes resulting from various impairments, such that a change in a particular effect will alter a measured parameter. This can employ: (i) optical techniques to monitor changes in a radio frequency (RF) tone power or in the spectral channel power distribution [3], or (ii) electrical post-processing techniques in the specific case of coherent detection [4]. The optical approaches have been shown to be powerful for OPM. However, the electrical distortions that are crucial for the signal quality at the decision point tend to be neglected in the optical approaches. Techniques proposed for OPM using off-line digital signal processing of received electrical data signals include the use of (i) amplitude histograms, power distributions, and asynchronous sampling to estimate bit error rate (BER) [5-8]; (ii) delay-tap plots to distinguish among impairments [9-12]; and (iii) pattern recognition techniques to identify multiple impairments [13, 14]. Recently, we have proposed a neural network approach to train receivers in an optical network to distinguish among resultant shapes of either the data channel’s eye diagrams or asynchronous delay-tap plots in the presence of the degrading effects of optical signal-to-noise ratio (OSNR), chromatic dispersion (CD), and polarization-mode dispersion (PMD) [15, 16].

In this paper, we experimentally compare the use of artificial neural networks (ANNs) trained with parameters derived from both delay-tap plots and eye diagrams to simultaneously identify OSNR, CD and PMD in a 40-Gbit/s non-return-to-zero on-off keying (NRZ-OOK) system. The monitoring range is 18-30 dB for OSNR, 0-100 ps/nm for CD, and 0-10 ps for differential group delay (DGD), i.e. first order PMD. A correlation coefficient of 0.995 is obtained when using delay-tap plots. This method exhibits slightly better performance compared with using eye diagrams, where a correlation coefficient of 0.972 is achieved.

2. Concept

With asynchronous delay-tap sampling, each sample point is comprised of two measurements separated by a specific time corresponding to the length of the delay [9]. Fig. 1 (a) illustrates one-half bit-period ($B/2$) delay-tap plots for a 40-Gbit/s NRZ-OOK signal at a few select combinations of OSNR, CD and DGD. Fig. 1 (b) shows the eye diagrams with slightly different combinations of impairments. Visually, it is obvious that these impairments produce distinct features in both the delay-tap plots and eye diagrams.

To simultaneously quantify the impairments, we use ANNs trained with parameters derived from delay-tap plots or eye diagrams. ANNs are information-processing systems that learn from observations and generalize by abstraction, which consist of multiple layers of processing elements called neurons [17]. Each neuron is linked to other neurons in neighboring layers by varying coefficients, as shown in Fig. 1 (c). ANNs learn the relationships among sets of input-output data that are characteristic of the device or system under consideration. After the input

vectors are presented to the input neurons and output vectors are computed, the ANN outputs are compared to the desired outputs and errors are calculated. Error derivatives are then calculated and summed for each weight until all of the training sets have been presented to the network. The error derivatives are used to update the weights for the neurons, and training continues until the errors reach prescribed values. After training, the ANN can be tested by use of other sets of data.

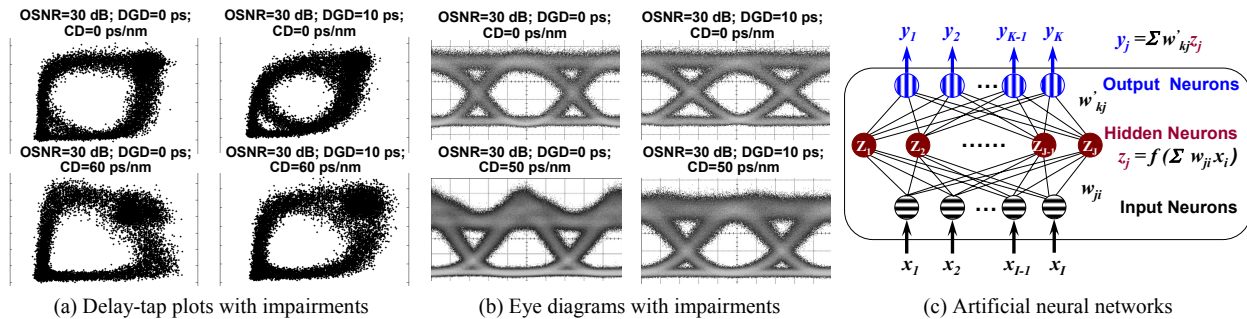


Fig. 1: Concepts of delay-tap plots, eye diagrams, and artificial neural networks.

3. Experiment Setup and ANN Models

Fig. 2 shows the experimental setup. The 40-Gbit/s NRZ-OOK signal is generated using a Mach-Zehnder modulator (MZM), driven by a 40-Gbit/s pseudo-random bit sequence (PRBS). The signal then goes through a DGD emulator, followed by a tunable dispersion compensating module (TDCM), which serves as the CD emulator. The DGD emulator has a range of -50 to +250 ps with a resolution of 0.002 ps, and the TDCM has a tuning range of +/- 400 ps/nm and a 10 ps/nm tuning resolution. The output of the TDCM is sent to an erbium-doped fiber amplifier (EDFA) with a variable optical attenuator (VOA) in front to adjust the received OSNR. The noise-loaded signal is then filtered by a bandpass filter (BPF) with 1 nm bandwidth, and sent to a sampling oscilloscope, where the waveform of the signal is recorded. The delay-tap asynchronous plots and eye diagrams can then be constructed prior to the parameters being extracted. In our experiment, we vary OSNR, CD and DGD to get a set of 252 waveforms (OSNR (dB): 18-30 in steps of 2; CD (ps/nm): 0-100 in steps of 20; DGD (ps): 0-10 in steps of 2), of which 137 combinations are used for training and 115 combinations are used for testing.

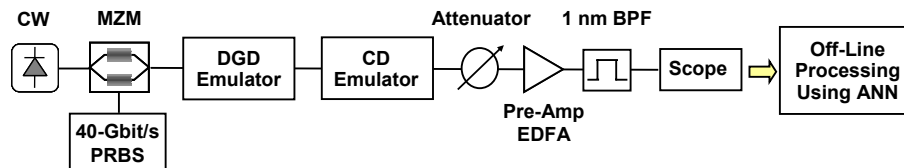


Fig. 2: Experimental setup. CW: continuous wave; MZM: Mach-Zehnder modulator; BPF: bandpass filter.

To quantify the distinct features, we derive parameters from the diagrams. For eye diagrams, we utilize widely-used parameters such as extinction ratio, Q-factor, crossing amplitude, eye height, jitter, and eye width [18]. For delay-tap plots, we divide the plots into four quadrants Q1-Q4 [16]. The data pairs are divided into the quadrants as follows: $(x_i, y_i) \in Q1$ if $\{0 \leq x_i \leq \text{Max}(x)/2 \text{ and } 0 \leq y_i \leq \text{Max}(y)/2\}$; $(x_i, y_i) \in Q2$ if $\{0 \leq x_i \leq \text{Max}(x)/2 \text{ and } \text{Max}(y)/2 < y_i \leq \text{Max}(y)\}$; $(x_i, y_i) \in Q3$ if $\{\text{Max}(x)/2 < x_i \leq \text{Max}(x) \text{ and } \text{Max}(y)/2 < y_i \leq \text{Max}(y)\}$; and quadrant 4 is not used since it contains data that is the mirror image of quadrant 2. Fig. 3 (a) illustrates this concept. With three quadrants defined, we can perform some basic statistical calculations on the data within each quadrant, such as means and standard deviations. For quadrants 1 and 3, we calculate the means and standard deviations of the magnitudes $(\bar{r}_1, \sigma_{r1}, \bar{r}_3, \sigma_{r3})$. For quadrant 2, we calculate the means and standard deviations of the x 's and y 's separately since this quadrant is on the off-diagonal. For the purpose of training our ANNs, we do not make use of the second quadrant's standard deviations since they do not vary significantly with different combinations of impairments. One final parameter we make use of is similar to the Q-factor, which we define as $Q_{31} = (\bar{r}_3 - \bar{r}_1) / (\sigma_{r1} + \sigma_{r3})$. The ANN using delay-tap parameters consists of seven inputs $(\bar{r}_1, \sigma_{r1}, \bar{r}_3, \sigma_{r3}, \bar{x}_2, \bar{y}_2, Q_{31})$, three outputs (OSNR, CD, and DGD), and 28 hidden neurons, which is illustrated in Fig. 3 (b). Similarly, a block diagram for the ANN using eye diagram parameters is shown in Fig. 3 (c).

The training errors of the ANNs were 0.0309 and 0.1147 for the case of using parameters derived from delay-tap plots and eye diagrams, respectively. The ANNs were trained by use of a software package developed by Zhang et al. [19]. Although alternatives were explored, a conjugate-gradient technique was chosen since it offers a nice

compromise in terms of memory requirements and implementation effort.

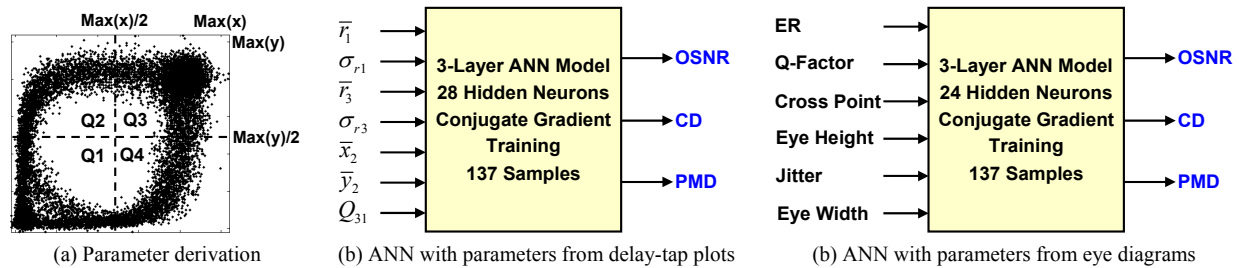


Fig. 3: Parameter derivation and ANN block diagrams. ER: extinction ration.

4. Experimental Results and Discussions

Once the models were trained, we validated their accuracies with a different set of 115 combinations as testing data. The software reported a correlation coefficient of 0.995 when using the parameters derived from delay-tap plots and 0.972 in the case of using eye-diagram parameters. The results are shown in Figs. 4 (a) and (b), respectively. When parameters from delay-tap plots were used, the root-mean-square (RMS) errors were 0.919 dB for OSNR, 6.368 ps/nm for CD, and 1.479 ps for DGD; when the parameters from eye diagrams were used, the RMS errors were 0.866 dB for OSNR, 14.642 ps/nm for CD, and 2.479 ps for DGD. In this particular case, results were slightly better when using parameters from the delay-tap plots. Fig. 4 (c) summarizes and compares the two cases.

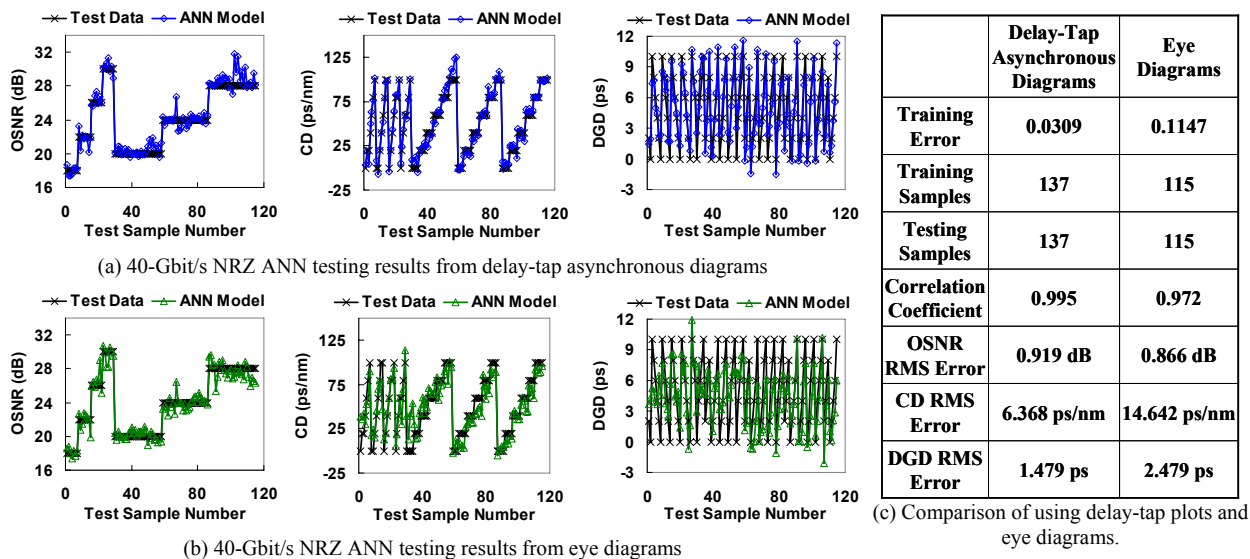


Fig. 4: Experimental results.

5. Conclusions

We have shown that ANN models trained with parameters derived from both measured delay-tap plots and eye diagrams can effectively be used to simultaneously identify levels of OSNR, CD, and DGD for 40-Gbit/s NRZ-OOK signals.

This work is supported by the U.S. Department of Commerce and the DARPA CORONET program, and is not subject to U.S. Copyright. The authors thank Jeng-Yuan Yang and Xue Wang from USC for their help.

6. References

- [1] D. C. Kilper et al, *JLT* 22 (1), 294-304 (2004).
- [2] Y. C. Chung, *ECOC '08*, paper We.1.D.1.
- [3] T. Luo et al, *OFC'03*, paper ThY3.
- [4] H. Sun et al, *Opt. Express* 16 (2), 873-879 (2008).
- [5] I. Shake et al, *Electron. Lett.* 34 (22), 2152-2154 (1998).
- [6] N. Hanik et al, *Electron. Lett.* 35 (5), 403-404 (1999).
- [7] S. Ohteru et al, *PTL* 11 (10), 1307-1309 (1999).
- [8] I. Shake et al, *JLT* 22 (5), 1296-1302 (2004).
- [9] S. D. Dods et al, *OFC'06*, paper OThP5.
- [10] S. D. Dods et al, *OFC'07*, paper OMM5.
- [11] B. Kozicki et al, *Opt. Express* 16 (6), 3566-3576 (2008).
- [12] B. Kozicki et al, *J. Opt. Netw.* 6 (11), 1257-1269 (2007).
- [13] R. A. Skoog et al, *PTL* 18 (22), 2398-2400 (2006).
- [14] T. B. Anderson et al, *JLT* 27 (16), 3729-3736 (2009).
- [15] X. Wu et al, *JLT* 27 (16), 3580-3589 (2009).
- [16] J. A. Jargon et al, *OFC'09*, paper OThH1.
- [17] M. H. Hassoun, the MIT Press (1995).
- [18] J. A. Jargon et al, *JLT* 26 (21) 3592-3600 (2008).
- [19] "NeuroModeler, ver. 1.5," Q. J. Zhang, et al (2004).